



Research article

Semi-automated detection of ungulates using UAV imagery and reflective spectrometry

Meyer E. De Kock^{a,b,*}, Václav Pohůnek^c, Pavla Hejmanová^a^a Czech University of Life Sciences Prague, Faculty of Tropical AgriSciences, Kamýcká 129, Praha-Suchbát, 165 00, Czech Republic^b University of Pretoria, Faculty of Veterinary Science, Onderstepoort, Pretoria, 0110, South Africa^c University of Chemistry and Technology, Department of Food Preservation, Technická 3, Praha 6, 160 00, Czech Republic

ARTICLE INFO

Keywords:

Automated detection
Aerial imagery
Arabian oryx
Drone
sRGB-colour profiles
UAV
Wildlife management

ABSTRACT

In the field of species conservation, the use of unmanned aerial vehicles (UAV) is increasing in popularity as wildlife observation and monitoring tools. With large datasets created by UAV-based species surveying, the need arose to automate the detection process of the species. Although the use of computer learning algorithms for wildlife detection from UAV-derived imagery is an increasing trend, it depends on a large amount of imagery of the species to train the object detector effectively. However, there are alternatives like object-based image analysis (OBIA) software available if a large amount of imagery of the species is not available to develop a computer-learned object detector.

The study tested the semi-automated detection of reintroduced Arabian Oryx (*O. leucoryx*), using the species' coat sRGB-colour profiles as input for OBIA to identify adult *O. leucoryx*, applied to UAV acquired imagery. Our method uses lab-measured spectral reflection of hair sample values, collected from captive *O. leucoryx* as an input for OBIA ruleset to identify adult *O. leucoryx* from UAV survey imagery using semi-automated supervised classification.

The converted mean CIE Lab reflective spectrometry colour values of $n = 50$ hair samples of adult *O. leucoryx* to 8-bit sRGB-colour profiles of the species resulted in the red-band value of 157.450, the green-band value of 151.390 and blue-band value of 140.832. The sRGB values and a minimum size perimeter were added as the input of the OBIA ruleset identified adult *O. leucoryx* with a high degree of efficiency when applied to three UAV census datasets.

Using species sRGB-colour profiles to identify re-introduced *O. leucoryx* and extract location data using a non-invasive UAV-based tool is a novel method with enormous application possibilities. Coat reflection sRGB-colour profiles can be developed for a range of species and customised to autodetect and classify the species from remote sensing data.

1. Introduction

Monitoring animals in their natural habitat is of critical importance in an environment prone to losing biodiversity (Jewell, 2013). The value of aerial surveys in wildlife monitoring is well known (Linchant et al., 2015), while the cost, safety and logistics usually limit the use of manned aircraft in this field of monitoring free-living animals in their environment. In the early 2000s, some of the first assessments using unmanned aerial vehicles (UAV) with imagery capture equipment for wildlife monitoring and surveying were done (Jones IV et al., 2006). Since then, the use of UAVs and their application in a range of survey

missions has increased. A larger range of species have been surveyed using UAVs in an ever-increasing range of environments and sensor types (Anderson and Gaston, 2013; Groom et al., 2013; Linchant et al., 2018; Watts et al., 2010). UAV-based data acquisition utilised for ungulates research has seen a rapid increase in the last few years where the majority focus on developing techniques on single species (Hu et al., 2020; Fritsch et al., 2021; Obermoller et al., 2021). UAV-based ungulate monitoring is not limited to the identification of species. Zoometric measurements can reveal additional information about the species that may include; an insight into the species' age structure (de Kock et al., 2021), growth rates (Christiansen et al., 2018), sex ratios, body

* Corresponding author. Czech University of Life Sciences Prague, Faculty of Tropical AgriSciences, Kamýcká 129, 165 00 Praha-Suchbát, Czech Republic.

E-mail address: dekock.meyer@up.ac.za (M.E. De Kock).

<https://doi.org/10.1016/j.jenvman.2022.115807>

Received 15 May 2022; Received in revised form 9 July 2022; Accepted 18 July 2022

Available online 6 August 2022

0301-4797/© 2022 The Authors. Published by Elsevier Ltd. This is an open access article under the CC BY license (<http://creativecommons.org/licenses/by/4.0/>).

condition (Krause et al., 2017) and behaviour (Torres et al., 2018).

Historically, during post-release monitoring of Arabian Oryx (*O. leucoryx*), the low-density distribution of these reintroduced animals results in a population size estimate with low accuracy (Zafar-Ul Islam et al., 2011). The difficult to navigate desert terrain *O. leucoryx* typically inhabits may have also had a negative impact on population estimates (Islam and Knutson, 2008). Recent studies proved the use of UAVs to monitor *O. leucoryx* can be a valuable tool for field biologists (de Kock et al., 2021). Because of the large amount of imagery collected during a UAV survey, the need arises for an automated process to identify the species of interest from UAV-based imagery (Corcoran et al., 2021).

Automated detection of wildlife from UAV-acquired imagery is dominated by the development of object detectors that are trained using convolutional neural networks (Kellenberger et al., 2017) and other variations of computer learning (Tuia et al., 2022; Zheng et al., 2021). The development of machine learning-based object detectors usually involves the labelling of the object of interest in a large number of images. These labelled objects are divided into test and train datasets that are used to train the detection model through computer learning software (Pathak et al., 2018). A large number of samples are needed to train the model efficiently. Low numbers of examples can be improved with data augmentation that can include mirroring, shifting and rotations. However, a low number of training examples can lead to over-fitting (Kellenberger et al., 2017).

Although artificial intelligence (AI) object detectors are available for a range of wildlife species, these detectors are usually developed from a horizontal perspective (Choiński et al., 2021) and detectors focused on imagery from a UAV vertical perspective usually requires a custom-trained detector. The conservation-based initiative (www.conservationai.co.uk) assists conservation-based researchers in the development of custom species detectors. This requires imagery of the species of interest to train and test the custom detector. An alternative when the required amount of imagery is not available of the species of interest to affectively train an object detector using deep learning is using extracted colour, texture and size values from biological samples to be used in supervised classification using object-based image analysis (OBIA) detection. This can be done by extracting the colour information from hair samples using reflective spectrometry. These colour values are used as inputs for the OBIA ruleset to perform a semi-automated supervised classification.

The use of reflective spectrometry, applied to remote sensing analysis is a relatively common practice (Herold et al., 2004). Uncommon, however, when used as an input for wildlife detection from imagery. With the advances in UAV sensors, the use of survey acquired imagery is more frequently applied in wildlife identification and management (Gonzalez and Johnson, 2017a; Hodgson et al., 2016; Linchant et al., 2015). In conservation management where monitoring is using UAV imagery, there is usually the need for the automatic detection of individuals or specific species (Chabot, 2009; Maire et al., 2015). Without automation, this process of a person looking at each image will be time-consuming and tedious. However, applying OBIA to UAV-acquired imagery to identify wildlife, the detectability, detection probability and limitations of this method are needed (de Kock et al., 2021). The use of lab-measured coat reflection is a novel research area that requires the adjustment of processes to align reflective spectrometry and OBIA. The conversion of data types generated by the reflective spectrometry analysis to be used in the digital environment of image analysis is a prerequisite.

OBIA classifies groups of pixels with similarities as input from the user together as an object and was primarily developed for remote-sensing data analysis where large data set are relatively common (Cai and Liu, 2013; Dingle Robertson and King, 2011). This method of classifying objects in imagery related to environmental studies has been used with great success (De Kock, 2015; Laliberte et al., 2010). OBIA uses a ruleset that includes a range of user-defined conditions as an input from the user, to perform a semi-automated supervised classification (Yu

et al., 2006). In this instance, automated detection focuses on the detection of individual animals (Singleton et al., 2010) by using the input from lab-measured coat reflection values to target a specific species. UAV acquired images in most instances collect location metadata that can be used to scale single images using the focal length and height or multiple images using photogrammetry. When this analysis is applied to scaled imagery, in addition to the objects identified, the process allows for a range of attribute information extraction e.g. location (X, Y and Z), size, height and colour values of the object (de Kock et al., 2021). This additional information enriches the census data, opening the door for additional data mining and spatial analysis (Yu et al., 2006).

Our study aims to investigate the application of animal coat spectral reflection to identify individual adult *O. leucoryx* using lab-measured reflectance of coat samples as an input for a semi-automated supervised classification using the colour values as an input for the OBIA ruleset.

We, therefore, aim to test the use of spectral reflection analysis values extracted from hair samples of captive *O. leucoryx*, as input for OBIA, to identify individual adult *O. leucoryx* from UAV based imagery. The first objective was to extract spectral reflection values from hair samples ($n = 50$) from captive *O. leucoryx*. Secondly, we investigated the conversion process of lab measured CIE Lab colour values to a compatible digital computer-based colour (sRGB) environment. Lastly, we tested the performance of the OBIA image extraction ruleset on a range of datasets acquired by UAV based image-capture survey of a protected area housing re-introduced *O. leucoryx*.

2. Materials and methods

2.1. Study species, site and samples

The *Oryx leucoryx* is classified in the genus *Oryx* and is the only within the genus with distribution out of Africa. Compared with the species within the *Oryx* genus, the overall size makes the *O. leucoryx* (Fig. 1A) the smallest. This medium-sized desert-dwelling antelope historically ranged over the Arabian Peninsula and as far north as Syria (Tear et al., 1997). The *O. leucoryx* was declared extinct in 1972 (Henderson, 1974) and through successful captive breeding programmes (Hatwood, 2017; Wilson and Price, 1994) the species was reintroduced (Daly, 1988; El Alqamy et al., 2008; Ostrowski et al., 1998; Price, 1989; Simkins, 2007) to their historical range. Post-release monitoring was identified as a critical management action to manage the species in protected areas (El Alqamy et al., 2008; Islam et al., 2011; Ostrowski et al., 1998).

Hair samples from the study herd ($n = 50$) were collected at Al Bustan Zoological Centre (lat 25.134944, long 55.881889), a conservation breeding centre, situated in Sharjah Emirate within the United Arab Emirates (UAE). The managed *O. leucoryx* population is housed as part of the regional captive conservation breeding programme of *O. leucoryx*. All individuals are handled yearly for routine veterinary checks that include: vaccinations, health checks, breeding access and separations, as per the best practice guidelines (De Kock et al., 2018). Hair samples of *O. leucoryx* older than ten months, the weight of sample < 3 g per individual, were collected from the back of each animal during this management process. The age parameter was added because of the change of the calf 'sand' colour (called 'الخطا') before the calf transforms to the white adult colour, which usually happens during the age of 2.5–8 months. The samples were collected from the full herd ($N = 61$) excluding individuals < 10 months ($N = 11$) of age. Each sample was stored separately and included attribute data of each individual that included the transponder identification number, age, sex and age and date of collection.

The outputs of hair sample analyses from the study herd were compared with datasets (Table 1) collected by UAV in the Dubai Desert Conservation Reserve (DDCR; lat 24.824789, long 55.657069). The DDCR is a 225 km² protected area in the Dubai Emirate in the UAE that

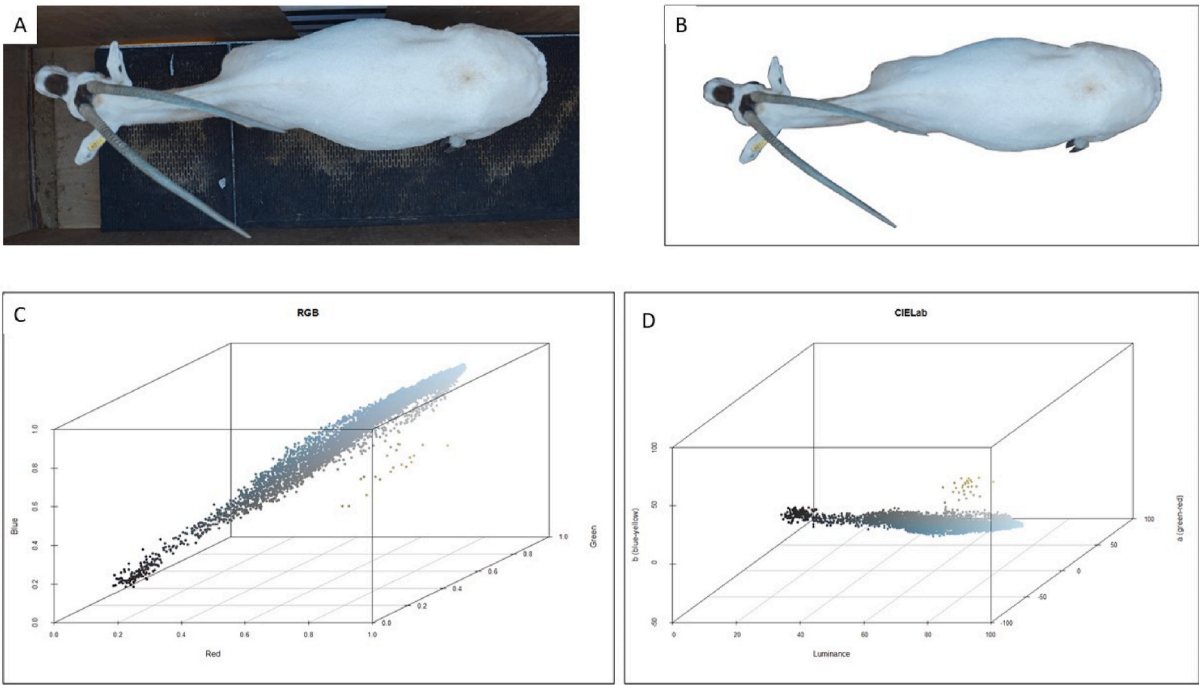


Fig. 1. A: An adult *O. leucoryx* top view. B: The *O. leucoryx* top view where the background was removed. C: The sRGB gamut represents the *O. leucoryx* as seen in B. D: The CIE Lab gamut represents the *O. leucoryx* as seen in B.

Table 1
UAV Survey datasets summary.

Survey Date	Animals identified	Time of day (UTM +4)	Lamination and conditions	Flight Time	Resolution	Sensor
March 4, 2018	72	10:34 a.m.–10:45 a.m.	Natural sunlight, No clouds	11 m 23 s	3.94 cm/pixel	1/2.3" CMOS Lens 20 mm f/2.8
March 18, 2018	56	09:38 a.m.–09:54 a.m.	Natural sunlight, No clouds	16 m 54 s	3.98 cm/pixel	1/2.3" CMOS Lens 20 mm f/2.8
October 14, 2018	47	08:55 a.m.–09:11 Am	Natural sunlight, Slight cloud cover	16 m 34s	3.98 cm/pixel	1/2.3" CMOS Lens 20 mm f/2.8

houses >800 reintroduced free-roaming *O. leucoryx* with the purpose of an *O. leucoryx* national and regional conservation plan.

2.2. Reflection spectrometry

Hair samples of 50 individuals from the captive study herd of *O. leucoryx* were analysed with the Konica Minolta CM-5 spectrophotometer (Tokyo, Japan). The sample quantity per animal was specified by the permit not to exceed 3 g of hair. The reflection was measured of each sample spread to cover the measurement window in a Petri dish. The Konica Minolta CM-5 built-in Petri dish calibration was activated for reflection analysis. Simulating daylight for digital analysis was considered, options include the D75 for ‘North Sky Daylight’, D65 ‘Average Daylight’ and D50 simulating ‘Noon sky Daylight’. D65 is a CIE standard illuminant that simulates mid-day daylight with a correlated colour temperature of 6504 K (Noboru and Robertson, 2005). The D65 best represents the high luminosity of a desert environment.

The spectrometer measures wavelengths of 360 nm–740 nm with a standard deviation within 0.1% (400 nm–740 nm). Each sample was measured three times with a slight adjustment of the sample to increase the variety of angles and the covering a more significant part of each sample during the analysis process. The data output was provided in a range of colour formats (CIE Lab, Hunters L, a, b; CIE XYZ) and wavelength-specific measurements.

2.3. Conversion of CIE lab to digital RGB

Although there is a standardised colour space with a wide gamut, the relatively narrow standardised RGB (sRGB) colour space resulted from the CIE Lab colour space conversion for inclusive digital representation was selected because the UAV sensor captured imagery in RGB format. The mean of the three readings of each sample was converted from CIE Lab to an RGB 8-bit digital value with a D65 setting. MATLAB (Natick, 2019) was used as a platform for the conversion following command `lab2rgb` (Mathworks, 2020).

The sRGB 8-bit converted colour values with the visualised colour in Table 2, show a colour value darker than expected when looking at the image of the *O. leucoryx* in Fig. 1A as well as dominated light grey colours in Fig. 1 to the earth colours in Table 2. This colour difference occurred because the hair samples were not washed before the spectrometry analysis. This is because the aim was not to determine the colour composition of the *O. leucoryx*’s coat, but to see the colour in real-world conditions as seen by UAV-based surveys. This may allow for environmental colour pollution like desert sand trapped between the hair.

The background (Fig. 1B) from the image was removed using the colour threshold analysis function in ImageJ®, Ver. 1.52a (Laboratory for Optical and Computational Instrumentation, University of Wisconsin, WI, USA). The processes allowed for the isolation of the *O. leucoryx* in the image in preparation for digital colour analysis.

Secondly, in Fig. 1 (C and D) the colour gamut is split into individual

Table 2

CIA Lab converted colour range to sRGB 8-bit range with 65% daylight as a white point. The range of each colour band is shown as a minimum, maximum and mean value. The RGB colour is a combination of each value combination. Brightness adjustment of sRGB values adding 55 to each 8-bit colour band as per equation 1.

CIE Lab (D65)	L	a	b
Min	45.02	-0.29	2.74
Max	75.54	1.72	9.9
Mean	62.82	0.323	6.33
sRGB (8Bit)	R	G	B
Min	108	106	102
Max	197	184	168
Mean	157.45	151.39	140.83
Standard Deviation	14.89	13.96	14.80
sRGB (8Bit)	R + 65	G + 65	B + 65
Min	168	166	162
Max	250	245	228
Mean	217.45	211.39	200.83

colours that represent the black of the horns and face markings, environmental pollution like desert sand and dirt trapped in the coat as the sandy colour, and the overall light grey representing the majority of the *O. leucoryx*'s body.

The RGB gamut does not have a specific band for brightness if compared to CIE Lab where the 'b' represents the brightness band, in sRGB this 'brightness' is generally incorporated in the respective RGB values by a higher value to represent an increase in 'brightness', among others. Adjusting brightness in sRGB is a complex adjustment depending on the required field of application (Bezryadin et al., 2007; Reinhard et al., 2002). The brightness adjustment was done using the Brightness modification of 8-bit sRGB values formula (Bezryadin et al., 2007) and resulted in the values shown in Table 2.

$$(R, G, B) = (r + M0, g + M0, b + M0)$$

Where 'r', 'g', 'b' values each respectively represent the 8-bit sRGB values. Where 'R', 'G', 'B' represent the adjusted sRGB 8-bit colour band values adjusted for brightness (Table 2).

Where M0 represents the respective sRGB value for brightness adjustment. The M0 was calculated using the brightness editing 'TV-based algorithm (Bezryadin et al., 2007) as 22% of the 8-bit colour value resulted in 55 that was added to each colour band.

2.4. UAV, sensors and control systems

During the data acquisition of the re-introduced *O. leucoryx* in the DDCR, the following UAV was used: the Ebee Plus (SenseFly, Switzerland) with a Canon S100 (Canon Inc., Japan) camera. The flight plan was developed in Pix4Dcapture (Ver 4.2.0) with a flight altitude of 90 m AGL and picture intervals with a subsequent 80% side- and 80% front overlap, with an orthophoto mosaic resolution of 3.98cm/pixel. Three flights of the study herd over different time periods: 4 -, March 18, 2018 and October 14, 2018, were surveyed and processed.

2.5. Photogrammetric processing and data analysis

The UAV acquired images with location data captured during the flight and written in the Exit header file of each image with the required overlap needed for photogrammetric processing. This processing of imagery to a georectified orthophoto mosaic was done using DroneDeploy online processing services (www.dronedeploy.com).

The processed imagery was added to eCognition Developer© v.9 (Trimble, USA), an OBIA software (Blaschke, 2010) where the data were analysed using a developed ruleset to extract adult *O. leucoryx* from the imagery using OBIA supervised classification. The 'Adult Arabian Oryx' ruleset, available under supplementary electronic material, provides

details on the segmentation process, object identification, class assignment and the export of the data.

The OBIA ruleset starts with the segmentation analysis, two segmentation processes were used. Firstly, the multiresolution segmentation and secondly the spectral deference segmentations analysis. The process divided the orthophoto mosaic into well-defined objects, including the *O. leucoryx*. Both analyses weighted the sRGB colour bands the same. The input for object classification was the three colour bands, sRGB ≥ minimum values identified in Table 2. The objects that met the bigger or equal to the set minimum values were classified. The classified object was filtered using a minimum size requirement of ≥50 pixels (3.98 cm/pixel) to refine the results. This minimum size of 199 cm² representing the 50 pixels is <10% of the drone footprint of adult *O. leucoryx* (de Kock et al., 2021). This allows for noise reduction to still identify *O. leucoryx* if the animal is partly obstructed, for example, by vegetation, during the survey.

Lastly, the identified object was exported as a smoothed polygon shapefile (.shp) with added attribute values that include the mean of each colour band and the total brightness represented in the object and the number of pixels represented in each object. The extracted shapes were exported as a polygon shapefile that includes data on the number of pixels within the polygon. This analysis was completed for a total of three sample data sets taken from the UAV imagery sample data of the protected area, and each sample set exceeds 1 km² in size.

The digital measurements in a comma-separated file format were exported as a dataset in R v3.6.2 (R_Core_Team, 2013). The dataset included all digital measurements as well as attribute data that included; the date, colour values, and the individual object size. The data structure was investigated and visualised using ggplot2 (Wickham, 2016), colour-distance (Weller, 2019) and colourspace (Ihaka et al., 2019) libraries.

The orthophoto mosaic imagery of each dataset and the OBIA vector files were added to ArcMap 10.7.1 (ESRI, Redlands, CA, USA) to visualise the results identified objects on the UAV-based orthophoto mosaics. In order to assess the accuracy of the applied OBIA ruleset results, the well-experienced rangers of Dubai Desert Conservation Reserve (DDCR) visually observed the herd during the UAV survey monitored and provide population numbers for each survey. In addition, the survey imagery was inspected visually to confirm the number of visible *O. leucoryx* in the survey data sets. In all three data sets the ranger survey data and the visual assessment correlated.

3. Results

The results of the spectral data analysis (Table 2) and the visualisation (Fig. 1) show the minimum, maximum and mean of each value in the CIE Lab and sRGB colour space of the adult *O. leucoryx* (n = 50) analysed hair samples. The converted mean CIE Lab reflective spectrometry colour values of the hair samples of adult *O. leucoryx* to 8-bit sRGB resulted in a Red value of 157.450, Green value of 151.390 and Blue value of 140.832 without the brightness adjustment. These sRGB values were added as an equal or larger than the cut-off colour value where all the objects with a combination of all three colour values, equal or higher than the cut-off values and a minimum size permitter were added as the input of the OBIA ruleset identified adult *O. leucoryx*. The use of the sRGB values without the brightness adjustment was selected to allow the ruleset a wider range in identification when imagery is underexposed and because there is no upper limit set for the ruleset, this will allow a wider range of detection when images are overexposed.

The OBIA 'Adult Arabian Oryx' results were applied to the three UAV-based survey datasets of the protected areas, as seen in Fig. 2. The OBIA ruleset identified adult *O. leucoryx* with a high degree of accuracy (Table 3), an average of 96.16% when applied to the three datasets.

The ruleset performed well in all three datasets that present different environmental conditions, and different times of the day and year. During visual result evaluation, the ruleset did not identify any *O.*

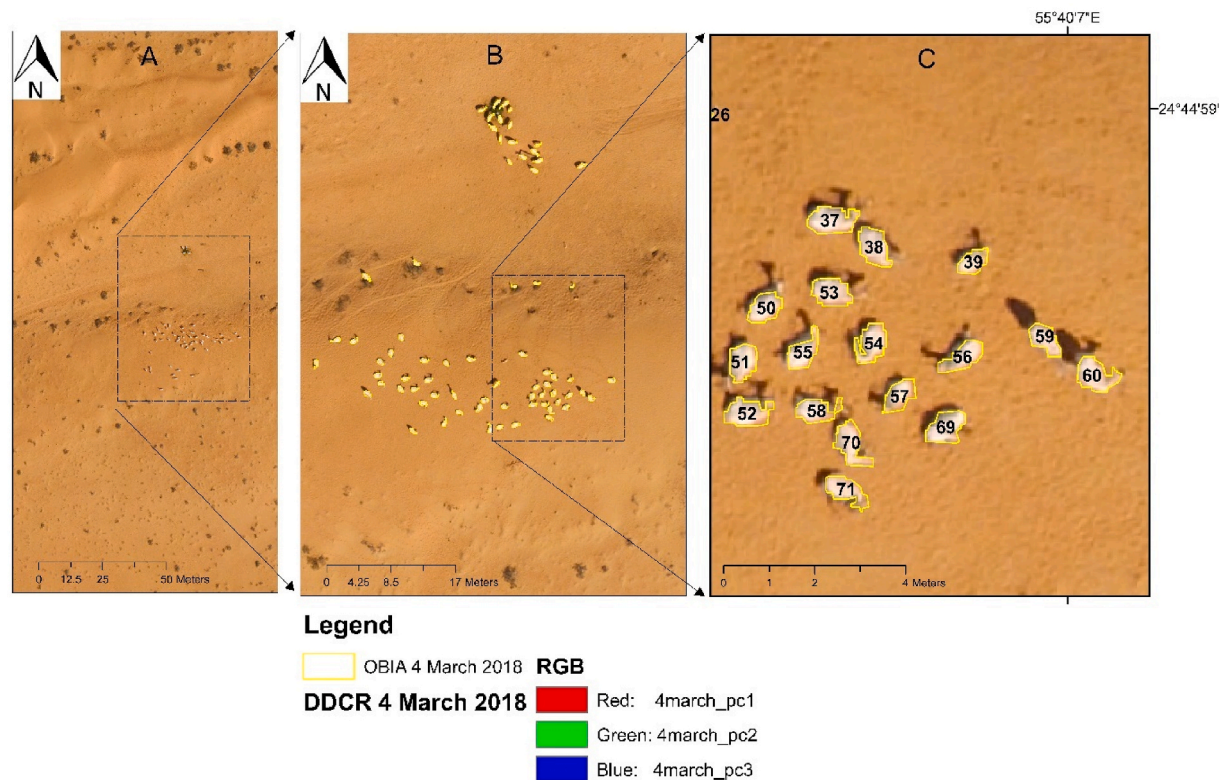


Fig. 2. The resulting output of the OBIA ruleset run on the UAV acquired data set of March 4, 2018. A: Show the processed imagery into an orthophoto mosaic. B: Shows the adult Arabian Oryx identified by OBIA (in yellow). C: Shows a closer view of the identified adult *O. leucoryx* with numbering labels. (For interpretation of the references to colour in this figure legend, the reader is referred to the Web version of this article.)

Table 3
The mean sRGB values and standard deviation of the object identified by ‘Arabian Oryx’ OBIA ruleset.

Dataset Date	Mean Red	Standard Deviation	Mean Green	Standard Deviation	Mean Blue	Standard Deviation	Total Oryx Identified	Total Objects
April 4, 2018	228.42	4.63	198.41	4.78	153.80	7.52	72	8561
April 18, 2018	230.46	4.37	199.99	6.81	154.56	7.56	56	2435
October 14, 2018	221.94	6.51	194.12	7.83	150.27	9.07	47	7131

leucoryx with the ‘sandy’ calf colour, as illustrated in Fig. 3 Left & Right - objects a. However, there was one false negative in two of the datasets (Fig. 3 Left-object B&C and 3 B – object B).

The OBIA software groups pixels of similar values together to represent objects. The results of the object identified in the three datasets (Tables 3 and 4) show the mean sRGB colour values.

In this case, although the OBIA ruleset identified the object, it failed to differentiate multiple objects, and this shortcoming is a segmentation issue rather than a final classification process. The failure to distinguish between numerous objects within the identified object will affect the survey’s overall accuracy, resulting in undercounting.

4. Discussion

Our study demonstrates the effective use of animal coat reflective spectrometry data as an input to OBIA to identify specific species from UAV base imagery, with good performance on the datasets. Similar UAV-based ungulate detection research using thermal imaging relies on manual measurements as an input for the manual classification of ungulates (Witczuk et al., 2018) compared to the semi-automated process developed. In addition, environmental conditions in arid regions like radial heat, humidity and dust (Pan et al., 2021) may influence the accuracy of thermal imaging. However, more data from a range of heterogeneous landscapes are needed to test the overall robustness and

performance of the OBIA ruleset. Habitats with more canopy cover may be challenging to survey, however, behavioural knowledge of the species of inters can provide criteria for a custom flight plan that capitalise on the best probability to capture images where canopy cover have a reduced impact on detection. An example of such behaviour can include preference on grazing, browsing and drinking times and avoiding survey flights during the heat of the day when the most animals are looking for shaded areas. The extracted reflective spectral data produced a species sRGB-colour profiles, this proof of concept has a range of practical applications where specific species can be targeted during the data analysis of UAV-based imagery.

If confounding factors like data quality are controlled the OBIA ruleset performs well, this can include the standardisation of the sensor and settings like white balance to name a few. There are, however, data inconsistencies that affect the overall efficiency of the OBIA ruleset to identify individual animals. The UAV-acquired imagery is processed by photogrammetry software, using multiple images taken during the survey, and turns it into a composite orthophoto mosaic. The combination of overlapping images in the photogrammetry process to produce a single ortho-rectified image presents complications with objects that move during or in-between images. This results in ‘ghost’ objects as seen in Fig. 3 Left object B and in extreme cases, the moving object between images can result in multiple representations of the same animal or no representation of the object in the final composite image. In addition,

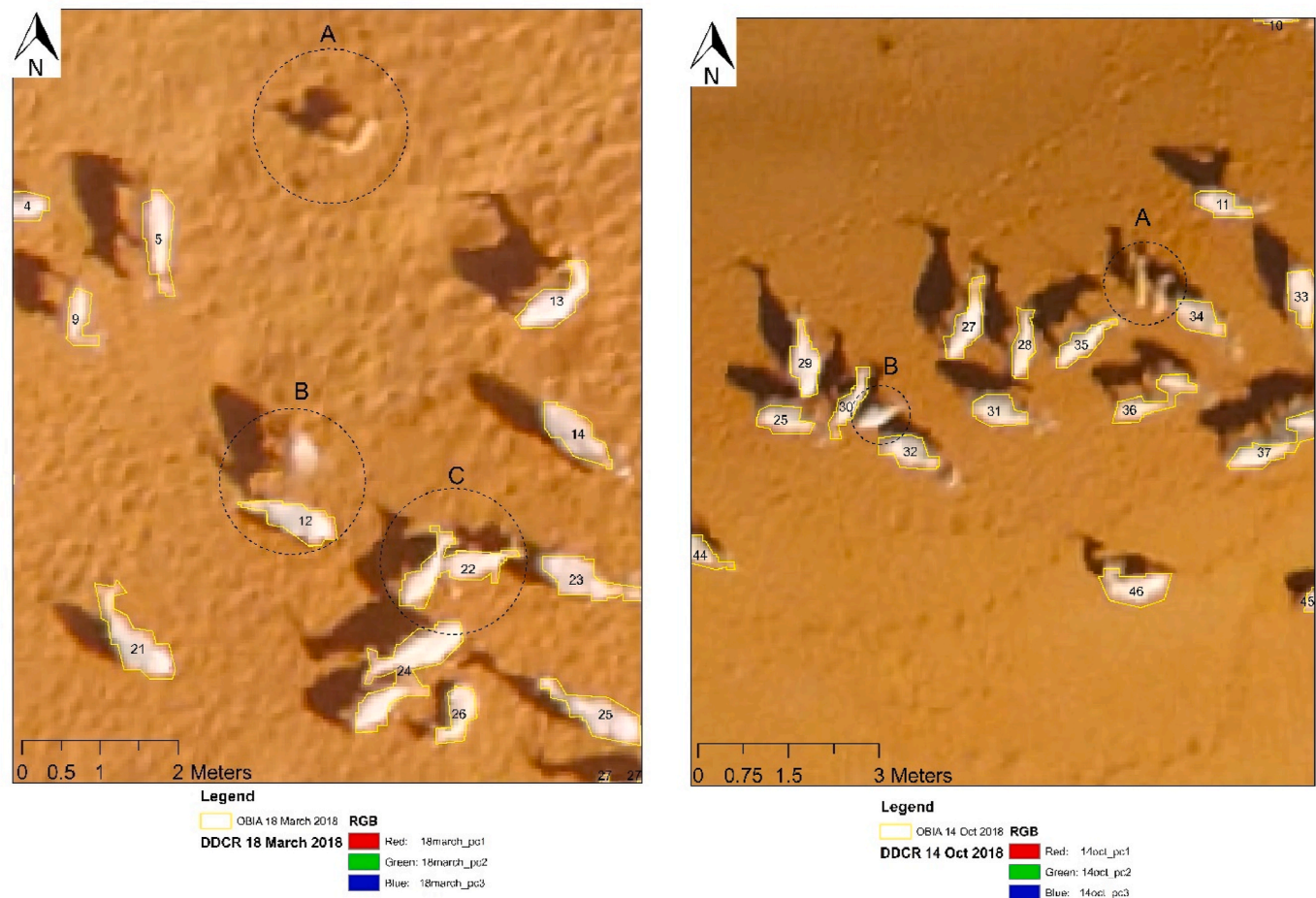


Fig. 3. Left: Identified adult *O. leucoryx* from the March 18, 2018 dataset. Object A- The *O. leucoryx* calves in their juvenile coat colour is not identified by the OBIA ruleset as an adult *O. leucoryx*. Object B- a ‘ghost image of an *O. leucoryx*, where the shadow is visible; however, the animal itself moved during or between overlapping images resulting in the ‘ghost’ image. Object C- Multiple objects identified as a single object. Right: Identified adult *O. leucoryx* from the March 18, 2018 dataset. Object A- The *O. leucoryx* calves still in their juvenile coat colour is not identified by the OBIA ruleset as an adult *O. leucoryx*. Object B- a ‘ghost image of an *O. leucoryx*, where the shadow is visible; however, the animal itself moved during or between overlapping images resulting in the ‘ghost’ image. . (For interpretation of the references to colour in this figure legend, the reader is referred to the Web version of this article.)

Table 4
Result of identified Adult *O. leucoryx* applying the OBIA ruleset: ‘Adult Arabian Oryx’ on all three datasets. The confusion matrix indicates the single polygons identified by the ruleset.

	Summery		April 4, 2018		April 18, 2018		October 14, 2018	
	Yes	No	Yes	No	Yes	No	Yes	No
Yes	175	0	72	0	56	0	47	0
No	2	18,127	0	8561	2	2435	0	7131

confounding factors can include a range of factors related to the UAV platform: stability, the selected flight plan; the sensor: sensor sensitivity, motion blur and the environment: vegetation cover, heterogeneous landscapes etc.

If there is no clearly defined boundary between objects of the same values specified in the ruleset, the objects will be grouped as a single object. This is observed in Fig. 3 Left object C, where two animals are close to each other with a limited background to clearly define the boundary and therefore result in a single object classification.

The significant differences in images representing *O. leucoryx* visible in Table 1, Figs. 1 and 3 show the influence of a non-standardised sampling technique where the sensor perimeters are automatically adjusted with limited supervised input. The influence of the variation of white balance settings between the survey data and the change in

lighting conditions on the survey dates results in a range of challenges during colour comparisons. Most off-the-shelf UAVs and sensors are programmed to produce a ‘beautiful photo’ with limited manual programming of the sensor, however, the automated setting adjustments of the sensor are negatively influenced by the automated gamma correction and white balance adjustment. Standardisation of the survey sensor, including the white balance (Seyednasrollah et al., 2019) can improve colour comparisons between datasets.

Ethical UAV-based wildlife surveys are paramount; however, these ethical standards are absent. Wildlife populations can respond idiosyncratically to UAV wildlife surveys, depending on a variety of factors (Hodgson and Koh, 2016). Although some countries did develop ethical protocols when using UAVs for wildlife surveys (Gonzalez and Johnson, 2017), ethical UAV wildlife survey operation is the main responsibility of the UAV pilot.

Automated wildlife detection from UAV-based imagery as a survey tool is a relatively new research area with a range of data extractions and analyses to investigate. The automated extraction of animals from photogrammetric-processed datasets includes spatial and temporal data. Additional data extraction of UAV-based animal surveys focuses on imagery baseline top view measurements applied to UAS-acquired imagery. This has a range of practical applications, which will increase with the addition of multiple UAV data acquisitions over set intervals e. g. seasonal. These time-specific dataset comparisons may include

calculations of survival rates of offspring, herd dynamics, and behavioural research.

5. Conclusions

When a field biologist applies UAV-based imagery to conservation planning it requires the coming together of three skillsets: ecology, drone hardware, and data interpretation. Often the technical know-how of data interpretation to use indicators in conservation planning is missing (De Kock and Gallacher, 2016). Creating an automated or semiautomated data extraction tool, in this case, an OBIA ruleset focus on the data extraction of adult *O. leucoryx* will assist field biologists during the technical data extraction process. Our study demonstrates that UAV-based monitoring combined with the OBIA ruleset to detect adult *O. leucoryx* can positively increase the accuracy of population estimates.

The case study can be adapted to a range of species by extracting baseline coat reflection values and integrating the results in a similar process. Monitoring ungulates in desert or similar, difficult-to-navigate and low canopy cover will be the best fitting for this developed method. The effect of climate change on desert ecosystems put a range of species at risk (Bombi et al., 2021) including endangered ungulates like addax (*Addax nasomaculatus*), scimitar-horned oryx (*Oryx dammah*) and dama gazelle (*Nanger dama*). Monitoring these species under environmental stress can be of great importance for conservation planning. The coat reflection data analysed to represent a species' sRGB-colour profiles can be added to the global species feature database initiative (Herberstein et al., 2022), known as "Animal Traits" (<https://animaltraits.org/>). The ability to focus the automated detection to recognise species' sRGB-colour profiles can be a valuable tool in a range of wildlife studies. However, this method is a tool that performs well in optimal conditions for this toolset. The sampling of captive animals and applying the results to a free-living population allows for a non-invasive automated survey technique. The conditions may include meteorological, environmental, surveyed species, UAV sensor, flight plan, photogrammetric processing and the UAV pilot, which may all affect the data quality and performance of this toolset.

Ethical statement

The hair samples of Arabian Oryx were transported from UAE to the Czech Republic with CITES permit number 19CZ030078, all samples were collected during routine animal management and health screening in the presence of a registered veterinarian.

Authors' contributions

M.D.K conceived the idea and collected the samples. M.D.K, with the assistance of V.P did the reflective spectrometry analysis. M.D.K performed the spatial analysis, colour conversion and OBIA ruleset development. M.D.K and P.H led the writing of the manuscript with input from V.P. All authors contributed critically to the final draft and gave final approval for publication.

Declaration of competing interest

The authors declare no conflict of interest.

Acknowledgement

The authors acknowledge the following support and contributions:

Research funding: The study was supported by the Czech University of Life Sciences Prague, projects CIGA 20185008 and IGA 20223106, and by the Ministry of Education, Youth and Sports, Czechia, grant number CZ.02.2.69/0.0/0.0/19_074/0016295.

We want to thank His Excellency Abdul Jaleel Al Balouki, owner of

Al Bustan Zoological Centre, Sharjah, UAE for his kind support. We also acknowledge the assistance and support of the Environmental Agency Abu Dhabi, UAE.

Appendix A. Supplementary data

Supplementary data to this article can be found online at <https://doi.org/10.1016/j.jenvman.2022.115807>.

References

- Anderson, K., Gaston, K.J., 2013. Lightweight unmanned aerial vehicles will revolutionize spatial ecology. *Front. Ecol. Environ.* 11, 138–146. <https://doi.org/10.1890/120150>.
- Bezryadin, S., Bourov, P., Ilinih, D., 2007. Brightness Calculation in Digital Image Processing, International Symposium on Technologies for Digital Photo Fulfilment. Society for Imaging Science and Technology, pp. 10–15.
- Blaschke, T., 2010. Object based image analysis for remote sensing. *ISPRS J. Photogrammetry Remote Sens.* 65, 2–16. <https://doi.org/10.1016/j.isprsjprs.2009.06.004>.
- Bombi, P., Salvi, D., Shuuya, T., Vignoli, L., Wassenaar, T., 2021. Climate change effects on desert ecosystems: a case study on the keystone species of the Namib Desert *Welwitschia mirabilis*. *PLoS One* 16 (11), e0259767. <https://doi.org/10.1371/journal.pone.0259767>.
- Cai, S., Liu, D., 2013. A comparison of object-based and contextual pixel-based classifications using high and medium spatial resolution images. *Remote Sensing Letters* 4, 998–1007. <https://doi.org/10.1080/2150704X.2013.828180>.
- Chabot, D., 2009. Systematic Evaluation of a Stock Unmanned Aerial Vehicle (UAV) System for Small-Scale Wildlife Survey Applications. McGill University.
- Choiński, M., Rogowski, M., Tynecki, P., Kuijper, D.P., Churski, M., Bubnicki, J.W., 2021. September. A first step towards automated species recognition from camera trap images of mammals using AI in a European temperate forest. In: International Conference on Computer Information Systems and Industrial Management. Springer, Cham, pp. 299–310. https://doi.org/10.1007/978-3-030-84340-3_24.
- Christiansen, F., Vivier, F., Charlton, C., Ward, R., Amerson, A., Burnell, S., Bejder, L., 2018. Maternal body size and condition determine calf growth rates in southern right whales. *Mar. Ecol. Prog. Ser.* 592, 267–281. <https://doi.org/10.3354/meps12522>.
- Corcoran, E., Winsen, M., Sudholz, A., Hamilton, G., 2021. Automated detection of wildlife using drones: synthesis, opportunities and constraints. *Methods Ecol. Evol.* 12, 1103–1114. <https://doi.org/10.1111/2041-210X.13581>.
- Daly, R.H., 1988. The early stages of re-introduction of the Arabian oryx in Oman. *Conservation and Biology of Desert Antelopes* 14–17.
- De Kock, M., Al Qarqaz, M., Burns, K., Al Faqeer, M., Chege, S., Lloyd, C., Gilbert, T., Alzahlawi, N., Al Kharusi, Y.H., Chuven, J., Javed, S., Al Dhaheri, S., 2018. Arabian Oryx Housing & Husbandry Guidelines. Environment Agency- Abu Dhabi (EAD), Abu Dhabi vol. 01.
- De Kock, M.E., 2015. Using Remote Sensing Data and Weighted Object-Based Image Analysis to Determine Animal Distribution. Master's thesis, University of Salzburg - UNIGIS).
- De Kock, M.E., Gallacher, D., 2016. From Drone Data to Decisions: Turning Images into Ecological Answers. *Innovation Arabia* 2016.
- de Kock, M.E., O'Donovan, D., Khafaga, T., Hejmanová, P., 2021. Zoometric data extraction from drone imagery: the Arabian oryx (*Oryx leucoryx*). *Environ. Conserv.* 1–6. <https://doi.org/10.1017/S0376892921000242>.
- Dingle Robertson, L., King, D.J., 2011. Comparison of pixel-and object-based classification in land cover change mapping. *Int. J. Rem. Sens.* 32, 1505–1529.
- El Alqamy, H., Kiwan, K., Al Daherie, A., 2008. Arabian Oryx project-UAE: one year of post release monitoring. In: Ninth Annual Sahelo-Saharan Interest Group Meeting, pp. 3–19.
- Fritsch, C.J., Hanekom, C., Downs, C.T., 2021. Hippopotamus population trends in ndumo game Reserve, South Africa, from 1951 to 2021. *Global Ecology and Conservation* 32. <https://doi.org/10.1016/j.gecco.2021.e01910>.
- Gonzalez, F., Johnson, S., 2017. Standard operating procedures for UAV or drone based monitoring of wildlife. In: Proceedings of UAS4RS 2017 (Unmanned Aircraft Systems for Remote Sensing). <https://doi.org/10.1080/01431160903571791>.
- Groom, G., Stjernholm, M., Nielsen, R.D., Fleetwood, A., Petersen, I.K., 2013. Remote sensing image data and automated analysis to describe marine bird distributions and abundances. *Ecol. Inf.* 14, 2–8. <https://doi.org/10.1016/j.ecoinf.2012.12.001>.
- Hatwood, M., 2017. Arabian oryx, Back from the Brink, Thanks to Zoos. AZA, Antelope and Giraffe TAG.
- Henderson, D., 1974. Were they the last Arabian oryx? *Oryx* 12, 347–350. <https://doi.org/10.1017/S0030605300011959>.
- Herberstein, M.E., McLean, D.J., Lowe, E., et al., 2022. AnimalTraits - a curated animal trait database for body mass, metabolic rate and brain size. *Sci. Data* 9, 265. <https://doi.org/10.1038/s41597-022-01364-9>.
- Herold, M., Roberts, D.A., Gardner, M.E., Dennison, P.E., 2004. Spectrometry for urban area remote sensing—development and analysis of a spectral library from 350 to 2400 nm. *Rem. Sens. Environ.* 91, 304–319. <https://doi.org/10.1016/j.rse.2004.02.013>.
- Hodgson, J.C., Baylis, S.M., Mott, R., Herrod, A., Clarke, R.H., 2016. Precision wildlife monitoring using unmanned aerial vehicles. *Sci. Rep.* 6, 22574. <https://doi.org/10.1038/srep22574>.

- Hodgson, J.C., Koh, L.P., 2016. Best practice for minimising unmanned aerial vehicle disturbance to wildlife in biological field research. *Curr. Biol.* 26, R404–R405. <https://doi.org/10.1016/j.cub.2016.04.001>.
- Hu, J.B., Wu, X.M., Dai, M.X., 2020. Estimating the population size of migrating Tibetan antelopes *Pantholops hodgsonii* with unmanned aerial vehicles. *Oryx* 54, 101–109. <https://doi.org/10.1017/S0030605317001673>.
- Ihaka, R., Murrell, P., Hornik, K., Fisher, J., 2019. 'colorspace': A Toolbox for Manipulating and Assessing Colors and Palettes.
- Islam, M.Z.-u., Ismail, K., Boug, A., 2011. Restoration of the endangered Arabian Oryx *Oryx leucoryx*, Pallas 1766 in Saudi Arabia lessons learnt from the twenty years of re-introduction in arid fenced and unfenced protected areas: (Mammalia: artiodactyla). *Zool. Middle East* 54, 125–140. <https://doi.org/10.1080/09397140.2011.10648904>.
- Islam, M.Z.U., Knutson, C., 2008. A Plan to Reduce the Risk of Mass Mortalities of Reintroduced Animals in the Mahazat As-Sayd Protected Area in Saudi Arabia.
- Jewell, Z.O.E., 2013. Effect of monitoring technique on quality of conservation science. *Conserv. Biol.* 27, 501–508. <https://doi.org/10.1111/cobi.12066>.
- Jones IV, G.P., Pearlstone, L.G., Percival, H.F., 2006. An assessment of small unmanned aerial vehicles for wildlife research. *Wildl. Soc. Bull.* 34, 750–758. [https://doi.org/10.2193/0091-7648\(2006\)34\[750:AAOSUA\]2.0.CO;2](https://doi.org/10.2193/0091-7648(2006)34[750:AAOSUA]2.0.CO;2).
- Kellenberger, B., Volpi, M., Tuia, D., 2017. Fast Animal Detection in UAV Images Using Convolutional Neural Networks, 2017 IEEE International Geoscience and Remote Sensing Symposium (IGARSS). IEEE, pp. 866–869. <https://doi.org/10.1109/IGARSS.2017.8127090>.
- Krause, D.J., Hinke, J.T., Perryman, W.L., Goebel, M.E., LeRoi, D.J., 2017. An accurate and adaptable photogrammetric approach for estimating the mass and body condition of pinnipeds using an unmanned aerial system. *PLoS One* 12, e0187465. <https://doi.org/10.1371/journal.pone.0187465>.
- Laliberte, A.S., Herrick, J.E., Rango, A., Winters, C., 2010. Acquisition, orthorectification, and object-based classification of unmanned aerial vehicle (UAV) imagery for rangeland monitoring. *Photogramm. Eng. Rem. Sens.* 76, 661–672. <https://doi.org/10.14358/PERS.76.6.661>.
- Linchant, J., Lhoest, S., Quevauxvillers, S., Lejeune, P., Vermeulen, C., Semeki Ngabinzeke, J., Luse Belanganayi, B., Delvingt, W., Bouché, P., 2018. UAS imagery reveals new survey opportunities for counting hippos. *PLoS One* 13, e0206413. <https://doi.org/10.1371/journal.pone.0206413>.
- Linchant, J., Lisein, J., Semeki, J., Lejeune, P., Vermeulen, C., 2015. Are unmanned aircraft systems (UAS s) the future of wildlife monitoring? A review of accomplishments and challenges. *Mamm. Rev.* 45, 239–252. <https://doi.org/10.1111/mam.12046>.
- Maire, F., Alvarez, L.M., Hodgson, A., 2015. Automating Marine Mammal Detection in Aerial Images Captured during Wildlife Surveys: a Deep Learning Approach, Australasian Joint Conference on Artificial Intelligence. Springer, pp. 379–385. https://doi.org/10.1007/978-3-319-26350-2_33.
- Mathworks, 2020. Convert CIE 1976 L*a*b* to RGB. User Guide (R2019a) Retrieved March 27, 2020 from: <https://uk.mathworks.com/help/images/ref/lab2rgb.html>.
- Natick, M., 2019. MATLAB R2019a Update 2 (9.6.0.1114505). The MathWorks Inc.
- Noboru, O., Robertson, A.R., 2005. 3.9: Standard and Supplementary Illuminants, Colorimetry. Wiley, Hoboken, NJ, USA.
- Obermoller, T.R., Norton, A.S., Michel, E.S., Haroldson, B.S., 2021. Use of drones with thermal infrared to locate white-tailed deer neonates for capture. *Wildl. Soc. Bull.* 45, 682–689. <https://doi.org/10.1002/wsb.1242>.
- Ostrowski, S., Bedin, E., Lenain, D.M., Abuzinada, A.H., 1998. Ten years of Arabian oryx conservation breeding in Saudi Arabia—achievements and regional perspectives. *Oryx* 32, 209–222. <https://doi.org/10.1046/j.1365-3008.1998.d01-38.x>.
- Pan, D., Jiang, Z., Maldague, X., Gui, W., 2021. Research on the influence of multiple interference factors on infrared temperature measurement. *IEEE Sensor. J.* 21 (9), 10546–10555. <https://doi.org/10.1109/JSEN.2021.3055757>.
- Pathak, A.R., Pandey, M., Rautaray, S., 2018. Application of deep learning for object detection. *Procedia Comput. Sci.* 132, 1706–1717. <https://doi.org/10.1016/j.procs.2018.05.144>.
- Price, M.R.S., 1989. *Animal Reintroductions: the Arabian oryx in Oman*. Cambridge University Press.
- R_Core Team, 2013. R: A Language and Environment for Statistical Computing. Foundation for Statistical Computing, Vienna, Austria.
- Reinhard, E., Stark, M., Shirley, P., Ferwerda, J., 2002. Photographic tone reproduction for digital images. In: Proceedings of the 29th Annual Conference on Computer Graphics and Interactive Techniques, pp. 267–276. <https://doi.org/10.1145/566570.566575>.
- Seyednasrollah, B., Young, A.M., Hufkens, K., Milliman, T., Friedl, M.A., Frolking, S., Richardson, A.D., 2019. Tracking vegetation phenology across diverse biomes using Version 2.0 of the PhenoCam Dataset. *Sci. Data* 6, 1–11. <https://doi.org/10.1038/s41597-019-0229-9>.
- Simkins, G., 2007. Re-introduction of Arabian Oryx into the Dubai Desert Conservation Reserve, Dubai, UAE Dubai Desert Conservation Reserve.
- Singleton, P.H., Lehmkuhl, J.F., Gaines, W.L., Graham, S.A., 2010. Barred owl space use and habitat selection in the eastern cascades, Washington. *J. Wildl. Manag.* 74, 285–294. <https://doi.org/10.2193/2008-548>.
- Tear, T.H., Mosley, J.C., Ables, E.D., 1997. Landscape-scale foraging decisions by reintroduced Arabian oryx. *J. Wildl. Manag.* 1142–1154. <https://doi.org/10.2307/3802112>.
- Torres, L.G., Nieuwkirk, S.L., Lemos, L., Chandler, T.E., 2018. Drone up! Quantifying whale behavior from a new perspective improves observational capacity. *Front. Mar. Sci.* 5, 319. <https://doi.org/10.3389/fmars.2018.00319>.
- Tuia, D., Kellenberger, B., Beery, S., Costelloe, B.R., Zuffi, S., Risse, B., Mathis, A., Mathis, M.W., van Langevelde, F., Burghardt, T., 2022. Perspectives in machine learning for wildlife conservation. *Nat. Commun.* 13, 1–15. <https://doi.org/10.1038/s41467-022-27980-y>.
- Watts, A.C., Perry, J.H., Smith, S.E., Burgess, M.A., Wilkinson, B.E., Szantoi, Z., Ifju, P.G., Percival, H.F., 2010. Small unmanned aircraft systems for low-altitude aerial surveys. *J. Wildl. Manag.* 74, 1614–1619. <https://doi.org/10.1111/j.1937-2817.2010.tb01292.x>.
- Weller, H., 2019. *Colordistance: Distance Metrics for Image Color Similarity*.
- Wickham, H., 2016. *ggplot2: Elegant Graphics for Data Analysis*. Springer-Verlag, New York.
- Wilson, A., Price, M.S., 1994. Reintroduction as a Reason for Captive Breeding, *Creative Conservation*. Springer, pp. 243–264. https://doi.org/10.1007/978-94-011-0721-1_12.
- Witezuk, J., Pagacz, S., Zmarz, A., Cypel, M., 2018. Exploring the feasibility of unmanned aerial vehicles and thermal imaging for ungulate surveys in forests-preliminary results. *Int. J. Rem. Sens.* 39 (15–16), 5504–5521. <https://doi.org/10.1080/01431161.2017.1390621>.
- Yu, Q., Gong, P., Clinton, N., Biging, G., Kelly, M., Schirokauer, D., 2006. Object-based detailed vegetation classification with airborne high spatial resolution remote sensing imagery. *Photogramm. Eng. Rem. Sens.* 72, 799–811. <https://doi.org/10.14358/PERS.72.7.799>.
- Zafar-Ul Islam, M., Ismail, K., Boug, A., 2011. Restoration of the endangered Arabian Oryx *Oryx leucoryx*, Pallas 1766 in Saudi Arabia lessons learnt from the twenty years of re-introduction in arid fenced and unfenced protected areas. *Zool. Middle East* 54 (Suppl. 3), 125–140. <https://doi.org/10.1080/09397140.2011.10648904>.
- Zheng, X., Kellenberger, B., Gong, R., Hajnsek, I., Tuia, D., 2021. Self-supervised pretraining and controlled augmentation improve rare wildlife recognition in UAV images. *Proc. IEEE Inter. Conf. Comp. Vision* 732–741.